University of Groningen

Molecular dynamics simulations of a fully hydrated dipalmitoyl phosphatidylcholine bilayer with different macroscopic boundary conditions and parameters

Tieleman, D. P.; Berendsen, H. J. C.

Molecular dynamics simulations of a fully hydrated dipalmitoylphosphatidylcholine bilayer with different macroscopic boundary conditions and parameters

D. P. Tieleman, and H. J. C. Berendsen

Molecular dynamics simulations of a fully hydrated dipalmitoylphosphatidylcholine bilayer with different macroscopic boundary conditions and parameters

D. P. Tieleman and H. J. C. Berendsen[a]

BIOSON Research Institute and Laboratory of Biophysical Chemistry, University of Groningen, Nijenborgh 4, 9747 AG Groningen, The Netherlands

We compared molecular dynamics simulations of a bilayer of 128 fully hydrated phospholipid (DPPC) molecules, using different parameters and macroscopic boundary conditions. The same system was studied under constant pressure, constant volume, and constant surface tension boundary conditions, with two different sets of charges, the single point charge (SPC) and extended single point charge (SPC/E) water model and two different sets of Lennard-Jones parameters for the interaction between water and methyl/methylene. Some selected properties of the resulting bilayer systems are compared to each other, previous simulations, and experimental data. It is concluded that in relatively high water concentration it is possible to use *ab initio* derived charges with constant pressure boundary conditions. The SPC water model gives a larger area per head group and a broader interface than the SPC/E model. Increasing the repulsion between water oxygens and CH_2/CH_3 groups has a large effect on the width of the interface and the area per head group. There is little difference between simulations with constant pressure and constant surface tension. The use of constant volume, using a reasonable estimate for the initial box dimensions, easily introduces artefacts. © *1996 American Institute of Physics.* [S0021-9606(96)51734-4]

I. INTRODUCTION

In the last few years a large number of theoretical studies on bi- and monolayers of biologically interesting lipids have appeared in the literature.[1,2] Such model systems for biomembranes can be studied in atomic detail with Monte Carlo, molecular dynamics, stochastic dynamics, or combinations of these techniques.

In the past studies of DPPC (dipalmitoylphosphatidylcholine) bilayers have been performed in our laboratory. Although these studies provided valuable insights into the structure of bilayers and transport properties of small molecules through the bilayer, progress in force field parametrization in the literature led us to reexamine the methods developed in the 1980s.[3–8] Recently Jakobsson and Scott reviewed some strategic issues in the simulations of lipid membranes.[9] They discussed different macroscopic boundary conditions and proposed simulations of bilayers under constant surface tension conditions.[9,10] Such an $N\gamma T$ ensemble would provide an alternative to the NPT and NVT ensembles customarily used in simulations. Different ensembles have also been studied by Feller *et al.*[11] and Zhang *et al.*[12]

One problem that arises in assessing the relative merits of each method, NPT, NVT, or $N\gamma T$, is the fact that typically data are compared from simulations with different parameters. Water–lipid ratios vary, force field parameters differ, there are temperature differences, and systems are of different sizes. This variety reflects the choices and tradeoffs that are necessary in any simulation of lipid layers, but makes direct comparison of methods complicated. This also applies to the force field, such as the choice of water model and specific interaction parameters.

Different approaches and parameters can be compared by doing a series of simulations in which parameters and boundary conditions are changed systematically, but doing this exhaustively is prohibitive in terms of computer time. In this study we present a set of simulations that differ from each other with respect to the macroscopic boundary conditions, water model, charges, and Lennard-Jones interaction parameters between carbons and water. We compare the simulations to determine the influence of these variables on a number of properties of bilayers that are likely to convey differences: the cell dimensions, density profiles across the interface, electrostatics, hydration of the lipid head groups, diffusion behavior, and order parameters.

II. METHODS

In one of the first studies of DPPC in atomic detail, a system containing 64 lipids and 736 waters adopted a gel phase at 335 K instead of a liquid crystalline phase ($L\alpha$).[5,8] To force the system into the $L\alpha$ phase three adjustments were made. The Lennard-Jones CH_2–CH_2 and CH_3–CH_3 interactions were modified, the GROMOS[13] dihedrals were replaced by Rychaert–Bellemans dihedral potential functions, and the charges on the head groups were divided by two to decrease the interactions between the head groups. This would compensate for a lack of dielectric screening because the water model used is not polarizable. However, such a reduction of charges is obviously not the most elegant solu-

[a]Author to whom correspondence should be addressed. Electronic mail: berends@chem.rug.nl

TABLE I. The two different sets of Lennard-Jones parameters for the CH_2/CH_3–Ow interaction. ϵ is in kJ/mol, σ in nm. The difference between the two sets is a higher repulsion between carbons and water oxygens in the second.

		ϵ	σ	Ref.
Set 1	CH_2–Ow	0.997	0.310	A in Ref. 14
	CH_3–Ow	1.201	0.310	
Set 2	CH_2–Ow	0.529	0.310	C in Ref. 14
	CH_3–Ow	0.637	0.310	

tion. In this section different modifications of the force field and boundary conditions are detailed and an overview of the simulations is given.

A. The force field

1. Charges

In a recent simulation, otherwise using the same parameters as in Ref. 8 Chiu *et al.* successfully used *ab initio* derived charges. We used both this new and the older set to compare them in the same system.

2. Lennard-Jones parameters for the water–methyl/methylene interaction

In previous simulations in our laboratory two different sets of Lennard-Jones parameters for the water–methyl/methylene interactions have been used: the parameters published in Ref. 8 (set 1 in Table I), also used by Chiu *et al.*, and a more recent set derived from a study of the decane–water interface[14] (set 2 in Table I). Van Buuren *et al.* examined five different values for the ϵ of Ow–CH_2 and Ow–CH_3 interactions because the original value from the GROMOS force field resulted in a solubility of decane in water that was far too high. Set 2 has been used in several recent lipid bilayer simulations.[7,15,16] The Ow–CH_2 and Ow–CH_3 interactions are expected to have a significant influence on the interface.

3. The water model

Several different water models have been used in simulations of lipid–water interfaces, most notably the single point charge (SPC),[17] extended single point charge (SPC/E) and TIP.[19] Although the differences in partial charges or geometry for one single molecule are small, they accumulate to give very noticeable effects on the total system.

Focusing on SPC and SPC/E, there are several reasons why one could prefer one over the other. SPC/E was originally developed because previous water models did not take into account the self-energy due to polarization.[18] SPC/E gives a better density, radial distribution function, self-diffusion constant, and dielectric constant[20] than SPC. Unfortunately, a model with as few parameters as SPC or SPC/E cannot exactly reproduce all experimentally observed values. The tradeoff for the improvements mentioned above

is that the thermodynamic potential for SPC/E is only correct if the proper polarization self-energy correction is applied. In simulations where water is in equilibrium in different environments such corrections cannot be applied and the effective free energy of SPC/E is too low (-27.6 kJ/mol), compared to -24.3 kJ/mol for SPC, the latter being close to the experimental value.[14,21] This means that the liquid state is thermodynamically too much favored for SPC/E. Since the solubility is important at interfaces, we have thus far used SPC for all interface studies from our laboratory.

4. The treatment of electrostatics

Electrostatic interactions require special care. In previous simulations from our laboratory a cylindrical cutoff[7,8,15,16,22] was used. Originally this method was used because it takes into account all electrostatic pair interactions. The electrostatic interactions within the cylinder were summed directly and the remaining part of the system was treated using an analytical solution of Poisson's equation. The contribution of this remaining part turned out to be negligible and was later eliminated. This method requires a cylindrical symmetry, making it undesirable for studying the interaction of bilayers with other molecules, and is expensive computationally.

Alternative methods include lattice-sum methods such as Ewald summation or particle–particle particle–mesh.[23–25] These methods have the disadvantage of enhancing artefacts caused by the periodic boundary conditions, which may or may not be of great importance. It is also not clear yet how to efficiently calculate the virial, which is needed to compute the pressure, when using lattice-sum methods.[9,26]

Another option is the use of stochastic boundary conditions with fast multipole expansion methods. This method has been utilized by Heller *et al.*[27] for a simulation of a system containing 200 POPC molecules.

For systems of lipids with neutral total charge a simple cutoff criterion for the electrostatics is most often used. It has been shown that cutoffs introduce artefacts in solutions with ions,[28] but if the cutoff is taken large enough (>1.8 nm), this method appears to work well for PC lipids.[9,29]

B. Macroscopic boundary conditions

Most molecular dynamics studies of biologically interesting lipid systems either use constant pressure (NPT)[6–8,15,16,22,30,31] or constant volume (NVT)[1,29,32–34] boundary conditions.

The first method allows the system to adjust the box sizes so that the internal virial matches the externally applied pressure.[35] This method has the great advantage that only an approximation of the initial sizes is needed, because the system will find its size by itself, based on the force field. Recently Chiu *et al.* introduced a surface tension into a simulation, on the assumption that the surface tension of a bilayer is twice that of a corresponding monolayer. This assumption is questionable on the grounds that the surface tension of a monolayer consists mainly of the surface tension of the alkane/air interface,[36–39] but it makes little difference simu-

lation wise: instead of isotropic pressure coupling one can couple anisotropically, with different pressure components in the plane of the bilayer and normal to the plane. When the interface is perpendicular to the z axis, the surface tension γ can be calculated[40] from

$$\gamma = -\int (p'(z) - p)dz, \qquad (1)$$

where $p'(z)$ is the lateral pressure, p the bulk pressure, and the integral is defined over the boundary layer. The integral can be extended to infinity, because $p'(z) = p$ in the bulk phase. With two interfaces perpendicular to the z axis, as in our case, this gives

$$\gamma = -\frac{1}{2}\left(\frac{p_x + p_y}{2} - p_z\right)L_z \qquad (2)$$

in which $p_\alpha = P_{\alpha\alpha}$ ($\alpha = x, y, z$) and L_z is the box length in the z direction. This results for a pressure of -100 bar in the x and y directions and a box length of 5.6 nm (as was used by Chiu et al.) in $\gamma = 28$ mN/m. Note that this value is half the value obtained by Chiu et al.[10] because we take into account two water–lipid interfaces (both sides of the bilayer). For a box length of ~6.7 nm, the same surface tension used by Chiu means a pressure of ~-80 bar in the x and y directions, which is the pressure used in all $N\gamma T$ simulations in this study.

Constant volume simulations require an accurate knowledge of properties such as the repeat distance from liquid crystals and the area per head group. Unfortunately, a wide range of values has been reported for these properties, and thus there is considerable uncertainty in these values. A system is likely to be forced into dimensions it would not assume by itself. This can lead to a high positive or negative internal pressure and to an unrealistic surface tension.

C. The simulations

All simulations were done with the GROMACS package,[26] on a parallel computer developed in our laboratory.

A starting configuration was created by placing DPPC molecules randomly rotated around their long axis on an 8×8 grid. The monolayer thus formed was copied to build a bilayer and the entire system was energy minimized. Water was added in a water/lipid ratio of 30.5 to 1 at a distance of 0.23 nm between water and any other atom, resulting in a system containing 128 DPPC molecules and 3910 water molecules, 18 130 atoms in total. The initial box sizes were $6.4\times6.4\times7.2$ nm, based on the box sizes obtained in a previous simulation (Ref. 22, system L) that used slightly different parameters. Note that the initial size is not critical when applying pressure coupling. The relatively large amount of water ($c = 0.43$ weight fraction water) leaves ample room for later studies on molecules that interact with the lipid bilayer and is expected to mimic a biological membrane better than a system with very little water. Experimental results suggest that DPPC bilayers in the $L\alpha$ phase are fully hydrated at $c = 0.36$[41,42] or $c = 0.40$,[43] both values below our water concentration.

TABLE II. Summary of the simulations performed. Column LJ indicates the set of Lennard-Jones parameters used for the Ow–CH$_2$ and Ow–CH$_3$ interaction (Table I). The first three used the charges in Ref. 8 (reduced), A–F the charges from Ref. 10 (full). Throughout this paper simulations will be referred to by the capital in the first column, amended by ensemble or water model for clarity.

System	LJ	Ensemble	Water model	Length (ps)
1	2	NPT	SPC	250
2	2	$N\gamma T$	SPC	250
3	2	NVT	SPC	250
A	2	$N\gamma T$	SPC/E	500
B	2	NPT	SPC/E	500
C	2	NVT	SPC/E	300
D	2	$N\gamma T$	SPC	500
E	2	NPT	SPC	500
F	1	NPT	SPC	500

The total system was energy minimized and run for 10 ps at constant volume to allow the water to adjust to the presence of the lipids. The final configuration of this run was used as starting point for simulations A and B.

In Table II an overview of the simulations is given. In the first three simulations we used the charges, bonded, and Lennard-Jones parameters as described in Ref. 8, with the parameters from the Cp simulation in Ref. 14, hereafter called set 2 (see Table I), and SPC water. In simulations A–C we used the same Lennard-Jones parameters, full charges, and SPC/E. In simulations D and E the same parameters were used as for simulations A–C, but with SPC instead of SPC/E. Finally, simulation F used the same parameters as E, but with the Lennard-Jones parameters from set 1.

The original starting configuration (A and B) had the same dimensions as the L run in Ref. 22 but the lamellar repeat distance in this system (7.1 nm) is somewhat high compared to experimental measurements. As a second starting structure an intermediate structure from simulation A was taken, with a repeat distance of 6.4 nm and an average head group area per lipid of 0.62 nm^2. This structure was used as a starting structure for simulations E and F, and after changing the box dimensions to $6.4\times6.4\times6.7$ nm also for the constant volume simulation C. This means a repeat distance of 6.7 nm, an average area per head group of 0.64 nm^2, and a density of 0.99 g cm^{-3}, which seem reasonable dimensions based on the experimental data for these values (see below).

All simulations were performed with temperature coupling[35] with a coupling constant $\tau = 0.1$ ps, on solvent and lipids separately, at 325 K. The transition temperature of DPPC for the transition between the gel and liquid crystalline phases is 315 K.[43] Pressure coupling[35] was used with a coupling constant $\tau = 1.0$ ps, at 1 bar in all three directions for NPT and at -80.0 bar in the x and y directions and 1.0 bar in the z directions for constant surface tension simulations. All bond lengths and water angles were restrained using SHAKE[44] with a relative tolerance of 10^{-5}. The time step

TABLE III. Repeat distances (d), average head group area (A), the average distance between the P atoms on both sides of the bilayer (P–P), and the width of the interface (IW), defined as the distance over which the water density drops from 90% to 10% of the bulk value. The repeat distances and head group areas for the NVT simulations are given solely for comparison. The experimental values are discussed in Sec. III.

System	Ens.	Water	d (nm)	A (nm^2)	P–P (nm)	IW (nm)
Expt.			6.7	0.62	3.7	...
A	$N\gamma T$	SPC/E	6.8	0.59	3.6	1.0
B	NPT	SPC/E	6.7	0.59	3.5	1.0
C	NVT	SPC/E	6.7	0.64	3.7	1.0
D	$N\gamma T$	SPC	6.6	0.61	3.5	1.2
E	NPT	SPC	6.7	0.60	3.6	1.2
F (set 1)	NPT	SPC	6.3	0.63	3.5	1.4

used was 2 fs. Intermediate structures were saved each 250 steps. A snapshot of the system is given in Fig. 1.

In all simulations presented here a twin-range cutoff of 1.0 nm/2.0 nm without shift or switch functions was used. Up to 1.0 nm all pair interactions were calculated, but between 1.0 and 2.0 nm only electrostatic interactions were taken into account using a list that was updated every 10 time steps (20 fs). In all simulations the same charge groups were used as in Ref. 10—the phosphatidylgroup and two groups containing half the glycerol backbone and one ester group.

III. RESULTS

A. Equilibration

There was a noticeable drift in the box sizes for simulations 1–3, even after 250 ps. After 250 ps the area per head group of system 1 was 0.52 nm^2, of system 2 it was 0.53 nm^2 and both were still decreasing. The interfacial width, defined as the distance over which the water density drops from 90% to 10% of the bulk value, in both cases was 0.5 nm, much too low for a realistic fluid phase DPPC bilayer. Obviously these systems were not in the right phase and apparently approaching a gel phase at 325 K. This is not an interesting phase for our purposes and only simulations A–F will be described below. After a period between 150 and 300 ps the box dimensions for all systems stabilized. The density profiles averaged over periods over 50 ps showed no significant differences after 200 ps and all analyses on systems A–F have been done on the last 100 ps of each trajectory.

In constant volume calculations, the pressure in the system can be taken as an indication of the correctness of the box size. The average (over all 300 ps) lateral and normal pressures in simulation G were −530 and −370 bar, respectively, and showed no drift during the simulation. These pressures correspond to a surface tension γ of 55 mN/m (or 55 dyn/cm), using Eq. (2).

B. Box and bilayer dimensions

A wide range of values for the average area/head group A per lipid and the repeat distance d in DPPC systems in the Lα-phase has been obtained from experiments, mainly x-ray

diffraction and nuclear magnetic resonance (NMR). From diffraction experiments, values for A of 0.663 nm^2,[42] 0.576 nm^2,[41] 0.709 nm^2,[45] and 0.665 nm^2[46] have been reported for fully hydrated DPPC in the Lα phase. The large range of these values is caused mainly by the uncertainty in determining the relevant amount of water in the lipid/water system. From NMR, reported values include 0.586 nm^2,[47] 0.56 nm^2,[48] 0.69 nm^2,[49] and 0.717 nm^2.[50] The four values are based on similar experimental results but on different interpretations of the data. Nagle has shown that all of these interpretations are questionable and has argued that the surface area per DPPC in a fully hydrated bilayer is 0.62 ± 0.02 nm^2.[51] A wide range of areas per lipid has been used in computer simulations as well. In recent constant volume simulations, values of 0.66 (Ref. 34) and 0.68 (Ref. 33) have been used for DMPC. Recent constant pressure simulations found values for DMPC or DPPC of 0.58,[10] 0.58 for a system with only 11 waters per lipid and 0.64 for a system with more water.[22]

In Table III the average area per head group for all simulations is given. There appears to be little effect of the surface tension on the area per head group. An anisotropic pressure of 100 bars clearly is not enough to have a significant influence on the average area. When comparing A and D, B and E, it appears that the use of SPC leads to a larger area per head group than SPC/E. This is consistent with the slightly higher charge of SPC/E, which causes SPC/E molecules to bind somewhat stronger to other SPC/E molecules compared to SPC. Upon changing the Lennard-Jones parameters from set 2 to set 1 the area per lipid increases. A lower repulsion between the carbon and waters leads to more water between the head groups and a swelling in the x and y directions. This is also apparent from the higher interfacial width in system F (Table III).

The multilamellar repeat distance d has been determined by diffraction as well. There is again a considerable spread in the results. Values of 6.0 nm have been reported for a fully hydrated bilayer at water concentration 0.40,[41,43,45] values of 6.7 nm at excess water in Refs. 42, 52, and 53 of 6.7 nm at $c=0.44$ by Lis et $al.$,[45] and of 6.5 nm by Gawrisch et $al.$[54] One reason for this large range is that phase separation occurs at higher water concentrations. In most cases a maxi-
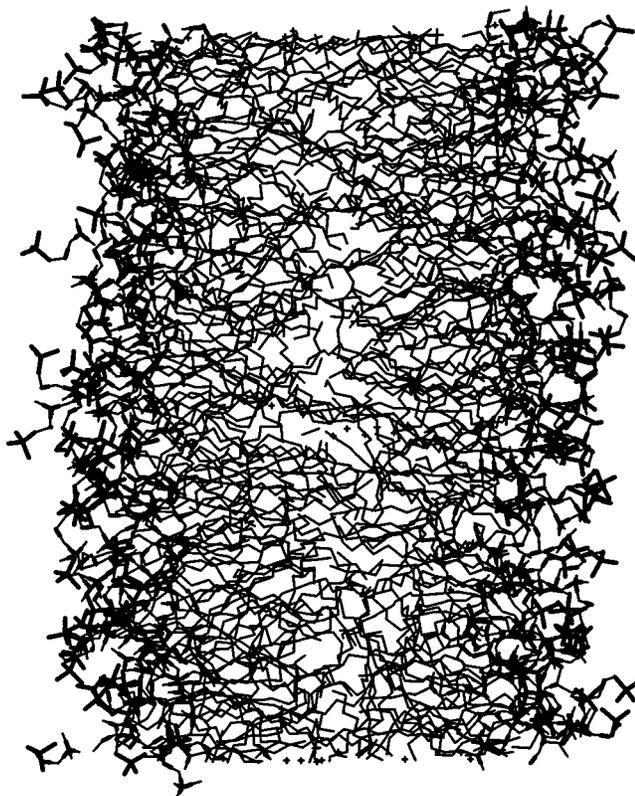
FIG. 1. Sideview of the bilayer. The choline group and the phosphorus atoms are plotted in bold. The water layer is not shown. The z axis runs across the bilayer.

mum repeat distance of 6.7 is reached, but the curve of d against water concentration is very steep for water concentrations c of about 0.40. Of course, in a molecular dynamics (MD) simulation the repeat distance will just continue to increase upon adding water. This makes it hard to compare the values found in MD simulations to experiments. Since the compressibility of a fluid is low, the repeat distance and average area per head group are not independent in simulations. The values for d (Table III) are consistent with the area per head group, assuming that the density for all simulations is approximately constant (Fig. 1).

C. Density profiles

The density profiles for all systems show similar behavior. There is a region of about 1.5 nm in which the system has the bulk density of water. Then the density rises at the interface, and drops toward the middle of the bilayer, consistent with neutron diffraction experiments and previous simulations. The maximum density reached is ~ 1.5 g cm^{-3}. This is slightly higher than observed in previous simulations and causes a total density of the systems with full charges (excluding F) of ~ 1.06 g cm^{-3}. The density in the system of Chiu *et al.* was slightly higher (calculated from the box dimensions and contents), consistent with a slightly higher lipid−water ratio.[10] In the systems with halved charges the density is around 1.00 g cm^{-3}, consistent with experimental values.[52]
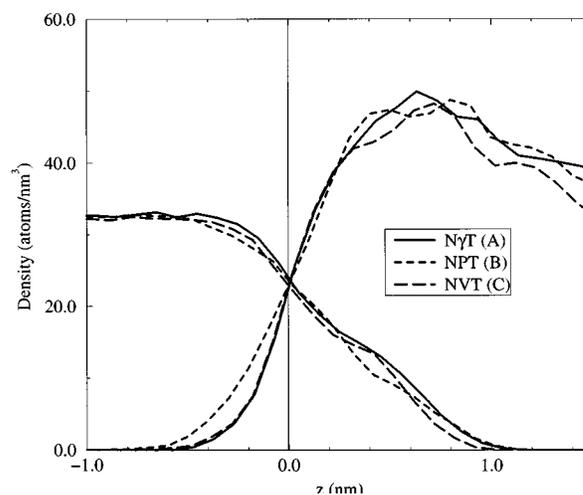

FIG. 2. The water–lipid interface for systems A–C (all using SPC/E). The zero of the x axis is defined as the point where lipid and water densities are equal. Data have been symmetrized over both sides of the bilayer. The water phase is on the left-hand side, the lipids on the right-hand side.

In Fig. 2, NPT, $N\gamma T$, and NVT simulations are compared (simulations A–C). There is little difference between the profiles for A and B. The NVT simulation C shows a lower density in the middle of the box, while the interface is comparable to simulations A and B. The tails must be oriented in such a way that they give the same density at the interface, for a larger area per head group. In Fig. 3 the electron density for systems B and C is plotted. Here it is clearer that the NVT system C has a much lower density in the middle of the bilayer. It appears that the system compensates for the fixed box sizes in the region with the lowest density (which is the most compressible), namely in the middle of the bilayer. In all three systems the interfacial width, defined as the distance over which the water density drops from 90% to 10% of the bulk value, is about 1.0 nm.
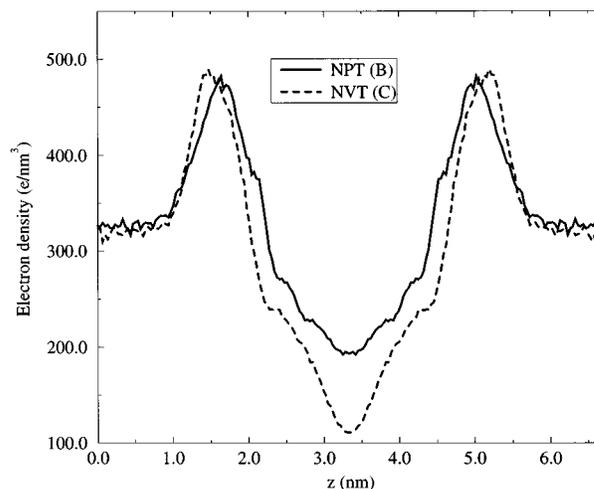

FIG. 3. Electron densities for systems B and C (both using SPC/E). Data have been symmetrized over both sides of the bilayer. Only nonhydrogen atoms have been used in the calculation. The interior of the bilayer is in the middle of the graph.
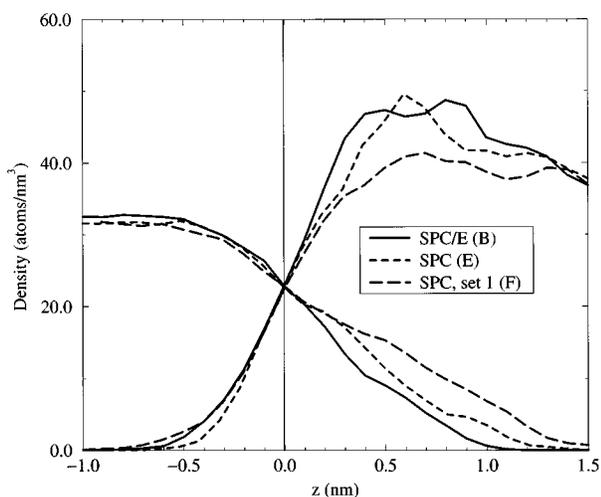
FIG. 4. The water/lipid interface for systems B, E, and F (all using NPT boundary conditions). The zero of the x axis is defined as the point where lipid and water have equal densities. Data have been symmetrized over both sides of the bilayer. The water phase is on the left-hand side, the lipids on the right-hand side.
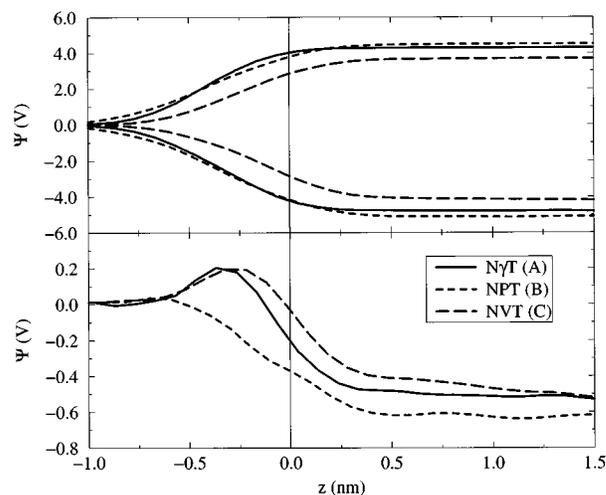

FIG. 5. The electrostatic potential in simulations A–C (all using SPC/E). Top: the contributions of DPPC and water to the potential. Potential zero was taken as the middle of the bilayer. The negative contributions come from the water molecules, the positive from DPPC. Bottom: the total potential across the interface. The water phase is negative with respect to the membrane interior. The zero point of the x-axis was defined in Fig. 2.

In Fig. 4 the interfacial region has been plotted for B (SPC/E), E (SPC), and F (set 1, SPC). The interface is broadest for F (1.4 nm), and smallest for B (1.0 nm). The use of SPC leads to a broader interface than SPC/E, reflecting the more favorable interaction between lipids and SPC. The use of set 1 LJ parameters leads to a significant broadening relative to the interface in E (set 2). This is consistent with previous simulations of the decane–water interface, in which set 1 allowed a considerable amount of mixing between decane and water.[14] It is also consistent with the width of 1.2–1.3 nm found by Chiu *et al.*, who used SPC/E combined with set 1. Interpretations of x-ray data also yield results of about 1.2–1.3 nm.[8,55] Wiener and White found a value of about 0.9 nm for DOPC at very low hydration (6 waters per lipid) and predicted higher values for higher hydration levels.[56]

The distance between the P atoms on both sides of the bilayer has been determined experimentally by Lewis and Engelman[46] and was found to be 3.7±0.1 nm. The values calculated from our simulations are given in Table III. In general, the values are a bit lower, 3.5 or 3.6 nm. Only the NVT simulation C yielded a value of 3.7 nm.

D. Electrostatics

The electrostatic potential across the box can be computed by doubly integrating the charge density $\rho(z)$

$$\psi(z) - \psi(0) = -\int_0^z dz' \int_0^{z'} \rho(z'') dz'' / \epsilon_\infty, \qquad (3)$$

where the position $z=0$ is taken as the middle of the bilayer interior, where $d\psi/dz=0$ because of symmetry.

For the dielectric constant in Eq. (3) we use the high-frequency value due to electronic polarization, taken equal to $2\epsilon_0$, where ϵ_0 is the vacuum permittivity. The effect of orientational polarization is already included in the value of ρ in which the partial charges are incorporated. In most previous

studies a value of 1 was taken for ϵ. This should be taken into account when comparing results with the results presented here.

Experimental measurements on PC/water interfaces yielded values from ~ -200 to as much as -575 mV for a DPPC–water bilayer.[54,57,58] In all cases the potential is negative in the water layer relative to the bilayer interior. Marrink *et al.* found positive values for two systems with different amounts of water.[22] This was believed to be an artefact of the simulation. With the improved parameters used in this study (full charges, more water), a value of about -250 mV is found.

In Fig. 5 the total potentials as well as the contributions from the lipids and water are plotted for the simulations A–C. In the NVT (C) and $N\gamma T$ (simulations A, D—not shown) simulations there is a positive peak of 50–100 mV before the total potential drops. Chiu *et al.* also observed a positive peak at the interface. This peak does not appear (or only weakly) in the other simulations. This might reflect small local changes at the interface due to the surface tension in these systems. The lower values for the lipid and water contributions to the potential in simulation C are probably also due to slightly different orientations of the head groups and the compensating water molecules at the interface (Fig. 6).

The potential in the systems B, E, and F (Fig. 6) correlates with the density profiles in Fig. 4. The smaller the interfacial width, the faster the potential reaches its maximum value. The lowest potential is found when using SPC/E, -312 mV.

E. Hydration at the interface

The radial distribution functions of water and lipid atoms gives information about the hydration of various parts of the
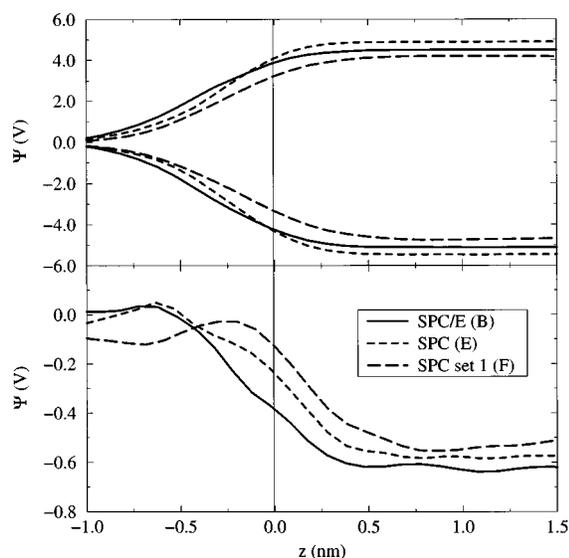
FIG. 6. The electrostatic potential in simulations B, E, and F (all using *NPT*). Top: the contributions of DPPC and water to the potential. Potential zero was taken as the middle of the bilayer. The negative contributions come from the water molecules, the positive from DPPC. Bottom: the total potential across the interface. The zero point of the *x* axis was defined in Fig. 4.

head groups. In Table IV the hydration numbers and the location of the first minimum are given for several head group atoms. Hydration numbers can be determined by integrating the radial distribution function to the first minimum.

The boundary conditions do not influence the hydration numbers. The water model does have a significant influence. For SPC/E the hydration numbers around the choline methyl groups are slightly lower than for SPC, reflecting the tendency of SPC/E water molecules to remain hydrogen bonded to other SPC/E waters. This effect becomes stronger deeper into the interface; the hydration of the phosphate group is ~10% higher in SPC than in SPC/E. The hydration numbers for system F are highest, because on average the lipids protrude further into the water layer.

F. Diffusion

From the mean square displacement in the *z* direction one can calculate the diffusion coefficient along the normal to the interface using the Einstein relation

TABLE IV. Hydration of choline–methyl groups, the $N(CH_3)_3$ group as a whole, the phosphate group and the two individual phosphate free oxygens. Values between braces are the locations of the first minimum in the radial distribution functions. In all cases there is a clear first minimum.

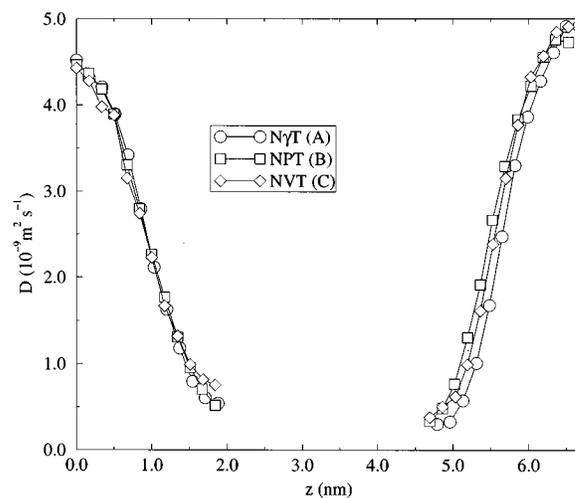| System	Waterm.	CH_3–Ow	$N(CH_3)_3$	P–Ow	pO–Ow
A	SPC/E	5.5(0.42)	15.2(0.57)	5.3(0.44)	1.5(0.32)
B	SPC/E	5.5(0.42)	15.2(0.57)	5.3(0.45)	1.5(0.32)
C	SPC/E	5.5(0.42)	15.1(0.57)	5.2(0.45)	1.50(0.32)
D	SPC	5.2(0.41)	15.3(0.57)	5.9(0.45)	1.5(0.32)
E	SPC	5.2(0.41)	15.5(0.57)	5.9(0.45)	1.5(0.32)
F (set 1)	SPC	5.6(0.41)	16.2(0.57)	6.1(0.45)	1.5(0.32)

FIG. 7. Diffusion constants for systems A–C (all using SPC/E). The hydrocarbon interior is in the middle of the graph. On the left-hand side the diffusion constant in the *z* direction is plotted, on the right-hand side the lateral diffusion constants. The data have been averaged over both sides of the bilayer.

$$D = \lim_{t \to \infty} \frac{1}{2t} \langle [z(t) - z(0)]^2 \rangle. \qquad (4)$$

In Figs. 7 and 8 the average lateral and normal diffusion coefficient have been plotted as function of the *z* position. The box was divided in 40 slabs. For each time origin all water molecules were then assigned to a slab. A diffusion coefficient per slab was calculated from the mean square displacement over 5 ps, using Eq. (4). Shorter periods than 5 ps give less accurate regression, longer periods allow too many water molecules to move out of the slab into another slab. The diffusion coefficient of SPC at 325 K is 6.2×10^{-9} m^2 s^{-1}, the diffusion coefficient of SPC/E at 325 K is
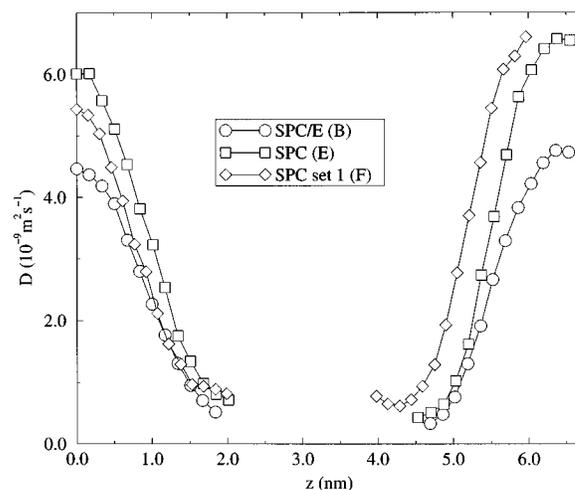

FIG. 8. Diffusion constants for systems B, E, and F (all using *NPT*). The hydrocarbon interior is in the middle of the graph. On the left-hand side the diffusion constant in the *z* direction is plotted, on the right-hand side the lateral diffusion constants. The data have been averaged over both sides of the bilayer.

4.4×10^{-9} m^2 s^{-1}. Both these values were calculated from a 200 ps run of 1728 water molecules, with temperature coupling ($\tau = 0.1$ ps, $T_{ref} = 325$ K), pressure coupling ($\tau = 0.5$ ps, $p_{ref} = 1.0$ bar), and a single cutoff of 1.0 nm. The diffusion coefficient of SPC/E is close to the experimental value, while the diffusion coefficient of SPC overestimates this value by a factor of 1.5.

In Fig. 7 the diffusion coefficients D in the z direction show that there is little difference between A and B, and only a small difference near the membrane interior for C. D decreases from the bulk value of 4.4×10^{-9} m^2 s^{-1} to approximately a value between 0.5 and 1.0×10^{-9} m^2 s^{-1} near the hydrocarbon interior. The lateral diffusion coefficients show similar behavior, but the maximum value is somewhat higher than the bulk value.

In Fig. 8 the normal and lateral diffusion coefficients have been plotted for the systems B, E, and F. The difference between E and H is caused by the difference in diffusion coefficient between SPC/E and SPC. In both systems the diffusion coefficients in the water phase are comparable to the values found in bulk water. In system B there is only a very small difference between the later and normal diffusion coefficients. This system has the broadest water phase. The lateral diffusion coefficient in system F is lower than in E, indicating more tightly bound water. The largest difference between the lateral and normal diffusion coefficients is also found in F. This corresponds with the low repeat distance for system F: there is only a very small layer of water, too small to observe diffusion characteristic of bulk water. It is interesting to note that the ratio of diffusion coefficients found in E and H remains approximately constant throughout the interfacial region. Although the self-diffusion coefficient of SPC/E is more realistic than that of SPC, this does not seem to lead to any qualitatively different behavior at the lipid/water interface.

G. Order parameters

The order parameters of the tails can be compared to values obtained from NMR on deuterated DPPC. The order parameter tensor S is defined as

$$S_{ij} = \tfrac{1}{2} \langle 3 \cos \theta_i \cos \theta_j - \delta_{ij} \rangle \tag{5}$$

in which θ_i is the angle the between the ith molecular axis and the bilayer normal. The brackets denote an ensemble average. The molecular axes for the nth CH$_2$ unit are z: vector from C_{n-1} to C_{n+1}, y: vector $\perp$ to z and in the plane through C_{n-1}, C_n, and C_{n+1}, x: vector $\perp$ to z and y.

From the diagonal elements S_{xx}, S_{yy}, and S_{zz} the deuterium order parameter S_{CD} can be calculated using

$$-S_{CD} = 2/3 S_{xx} + 1/3 S_{yy}. \tag{6}$$

Experimental values for $-S_{CD}$ for the fourth through the eighth CH$_2$ group are 0.20 ± 0.02.[51,59,60] For CH$_2$ groups toward the end of the tails the order parameter drops toward zero, indicating no preferential orientation.

Most simulation studies have reported values for $-S_{CD}$ close to 0.2.[1,8,10,33] Typically the general form of the order
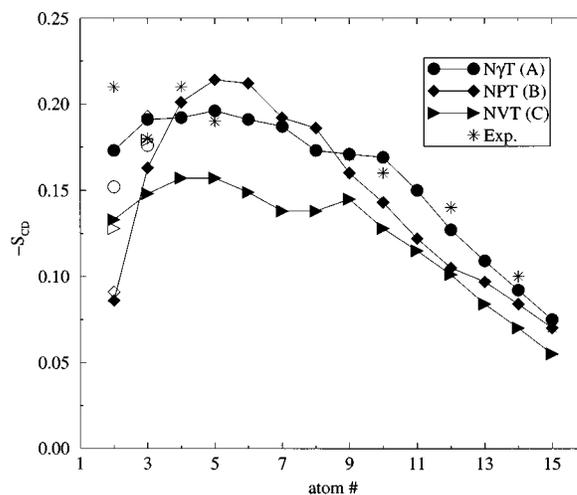

FIG. 9. Deuterium order parameters for three systems. Values have been averaged over both tails, except for carbons 2 and 3. Open symbols are for the sn 2 tail, closed for the sn 1 tail. Stars are experimental values from Ref. 6.

parameter profile is reproduced reasonably well. The order parameter profiles found in A and B fit this general pattern (Fig. 9). There is a plateau region extending over CH$_2$-groups 4–8, after which the values drop significantly. The largest differences are found for the first atom (the carbon next to the carbonyl carbon).

The order parameters for C are considerably lower. This confirms the observations made for the density profiles and electrostatic potentials that the structure of the interface for the NVT simulation differs significantly from the structure of the interface in the other simulations. Although the total lipid and water density is similar to that observed in A and B, the tails are less ordered along the axis normal to the bilayer, in order to fill the 0.64 nm^2 available per lipid. This is a serious artefact of the combination of force field parameters and macroscopic boundary conditions.

Also in system F the tails are less ordered than found in experiments (Fig. 10). The higher level of protrusion and the larger area per lipid seem to lead to a lower degree of ordering. The order parameters in system E are intermediary between B and F.

IV. DISCUSSION

Most properties of the systems with full charges analyzed in this study generally agree with previous simulations and with experiment. Although Egberts[8] obtained good agreement with experiments for his specific system and the same system was successfully used for the calculation of various transport properties, it does not provide a solid basis for further simulations on larger systems with more water at lower temperatures. Below we address each of the issues we raised.

A. *NPT, NVT,* or *NγT*

There are no significant differences in the results for NPT and $N\gamma T$ simulations. The size of the system is in all
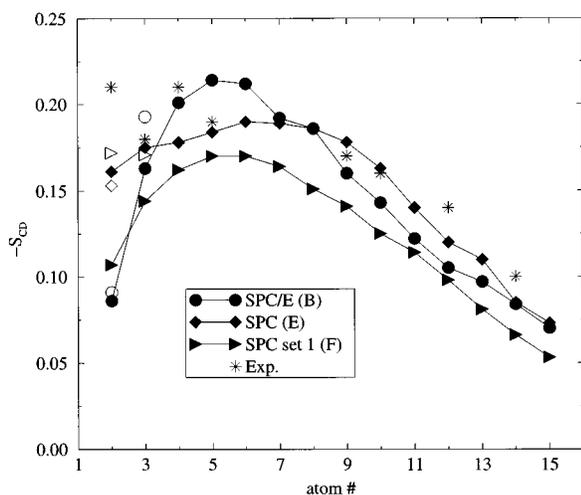
FIG. 10. Deuterium order parameters for three systems. Values have been averaged over both tails, except for the carbons 2 and 3. Open symbols are for the *sn* 2 tail, closed for the *sn* 1 tail. Stars are experimental values from Ref. 6.

cases approximately the same with or without surface tension, with otherwise the same parameters. The *NVT* simulation showed several serious artefacts, in spite of a careful initial guess of the box dimensions. The *NVT* system C has a much lower minimum density at the center of the bilayer and a different distribution behind the interface (at the side of the hydrocarbon interior) compared to the *NPT* and *NγT* simulations. The tails are considerably less ordered than is found experimentally.

We believe *NVT* is not very suitable for bilayers in biological systems because the fluidity makes it impossible or at least very hard to obtain accurate experimental values for the dimensions of the system. It is possible however to obtain good results from a constant pressure simulation without having to assume the presence of surface tension.

Anisotropic pressure coupling can lead to faster equilibration of a system, but there is no reason to use a specific value for this purpose, and much higher pressures might lead to the desired result (a good starting configuration) faster than pressures for which a physical justification can be given.

B. SPC or SPC/E

There is a significant difference in the results obtained with SPC or SPC/E. SPC/E leads to a sharper interface and a lower area per head group than SPC. In a bilayer system with enough water (in complete or almost complete hydration), a lack of screening of the dipoles of the lipids does not require the use of SPC/E.[10] The problems that led to the reduction of the charges in the head groups in Ref. 8 may well have been caused by the low amount of water per lipid. The diffusion coefficient of SPC remains higher than that of SPC/E throughout the system, but this does not lead to fundamentally different behavior.

In experimental work larger areas per lipid are typically found than in simulations. This is an argument in favor of

SPC, in spite of the considerable spread in the experimental values. The same holds for the width of the interface. SPC seems to lead to a width of the DPPC/water interface, defined as the distance over which the density of water drops from 90% to 10% of its bulk value, of about 1.2–1.3 nm, compared to a value of about 1.0 nm for SPC/E. There seems to be better experimental support for a value of ~1.2–1.3 nm.

In the end the choice between SPC and SPC/E still entails a tradeoff. This tradeoff is more important at interfaces between water and polar head groups than it is at interfaces between more hydrophobic molecules such as decane and water.[14] In the end, the better chemical potential of SPC and the apparently small influence of the better dielectric constant and diffusion coefficient of SPC/E seems to make SPC the better choice for interfaces. The better behavior in bulk water can only be combined with a proper chemical potential when a polarizable model is used: an effective pair potential always presents a compromise.

C. Lennard-Jones parameters and charges

The use of set 1 results in a broader interface and a higher area per head group than set 2. The order of the tails along the interface normal is less than found in experimental data. This set allows mixing of water and decane and the solvation of hexane in water, both of which are not consistent with experimentally measured solubilities of hexane and decane in water. If set 1 is used, it might compensate for other errors (such as wrong charges), but there is no good physical justification for its use. Egberts *et al.* published a complete force field for DPPC, including set 1.[8] This force field should be modified to use set 2.

Overall, the results of the simulations with full charges are good. Chiu *et al.* reported a generally successful simulation of a DMPC bilayer and the results obtained in this study depict a realistic fluid phase bilayer. One drawback of the full charges is the somewhat increased total density. The density might be improved by modifying other interaction parameters at the interface, but it seems questionable whether this is worth the effort. The most rigorous solution to improve the model would be the introduction of polarizability and a complete reparametrization of the force field.

V. CONCLUSIONS

Although choosing between the alternative parameters and boundary conditions discussed in this study will always mean a tradeoff, we draw the following conclusions. *Force field*: it is possible to use full charges in a system of fully hydrated lipids instead of the reduced charges used in previous studies from our laboratory. In the force field published in Ref. 8 the $Ow-CH_2$ and $Ow-CH_3$ Lennard-Jones interaction parameters should be changed to set 2. *Water model*: Although neither SPC nor SPC/E is perfect, generally it is better to use SPC in interface studies. *Macroscopic boundary conditions*: It makes little difference whether a surface tension or isotropic pressure is used. Constant volume simulations of lipid bilayers easily lead to serious artefacts.

ACKNOWLEDGMENTS

[1] R. Pastor and R. Venable, in *Computer Simulation of Biomolecular Systems: Theoretical and Experimental Applications*, edited by W. van Gunsteren, P. Weiner, and A. Wilkinson (Escom Science, Leiden, 1993), Chap. 2, pp. 443–464.

[2] Membrane Structure and Dynamics, edited by K. Merz and B. Roux (to be published).

[3] P. van der Ploeg and H. J. C. Berendsen, J. Chem. Phys. **76**, 3271 (1982), It should be noted that there is a significant typographic error in the paper. For both methylene and methyl σ should be $\sigma=0.374$ nm.

[4] P. van der Ploeg and H. Berendsen, Mol. Phys. **49**, 243 (1982).

[5] E. Egberts, Ph.D. thesis, University of Groningen, The Netherlands, 1988.

[6] E. Egberts and H. Berendsen, J. Chem. Phys. **89**, 3718 (1988).

[7] J. López Cascales, J. García de la Torre, S. Marrink, and H. Berendsen, J. Chem. Phys. **104**, 2713 (1996).

[8] E. Egberts, S. Marrink, and H. Berendsen, Eur. Biophys. J. **22**, 423 (1993).

[9] E. Jakobsson and H. Scott, in Ref. 2.

[10] S.-W. Chiu *et al.*, Biophys. J. **69**, 1500 (1995).

[11] S. E. Feller, Y. Zhang, and R. W. Pastor, J. Chem. Phys. **103**, 10267 (1995).

[12] Y. Zhang, S. E. Feller, B. R. Brooks, and R. W. Pastor, J. Chem. Phys. **103**, 10252 (1995).

[13] W. F. van Gunsteren and H. J. C. Berendsen, *GROMOS-87 Manual*, (Biomos BV, Nijenborgh 4, 9747 AG Groningen, The Netherlands, 1987).

[14] A. R. van Buuren, S. J. Marrink, and H. J. C. Berendsen, J. Phys. Chem. **97**, 9206 (1993).

[15] S. J. Marrink and H. J. C. Berendsen, J. Phys. Chem. **98**, 4155 (1994).

[16] S. J. Marrink, F. Jähnig, and H. J. C. Berendsen, Biophys. J. (in press).

[17] H. J. C. Berendsen, J. P. M. Postma, W. F. Gunsteren, and J. Hermans, *Intermolecular Forces*, edited by B. Pullman (Reidel, Dordrecht, 1981).

[18] H. Berendsen, J. Grigera, and T. Straatsma, J. Phys. Chem. **91**, 6269 (1987).

[19] W. L. Jorgensen, J. Am. Chem. Soc. **103**, 335 (1981).

[20] Y. Guissani and B. Guillot, J. Chem. Phys. **98**, 8221 (1993).

[21] J. Hermans, A. Pathiaseril, and A. Anderson, J. Am. Chem. Soc. **110**, 5982 (1988).

[22] S. Marrink, M. Berkowitz, and H. Berendsen, Langmuir **9**, 3122 (1993).

[23] R. W. Hockney and J. W. Eastwood, *Computer Simulations Using Particles* (McGraw-Hill, New York, 1981).

[24] B. A. Luty, I. G. Tironi, and W. F. van Gunsteren, J. Chem. Phys. **103**, 3014 (1995).

[25] T. Darden, D. York, and L. Pedersen, J. Chem. Phys. **98**, 10089 (1993).

[26] H. Berendsen, D. van der Spoel, and R. van Drunen, Comp. Phys. Comm. **91**, 43 (1995).

[27] H. Heller, M. Schaefer, and K. Schulten, J. Phys. Chem. **97**, 8343 (1993).

[28] P. Smith and W. van Gunsteren, in *Computer Simulation of Biomolecular Systems*, edited by W. van Gunsteren, P. Weiner, and A. Wilkinson (ESCOM Science, Leiden, The Netherlands, 1993), Vol. 2, pp. 182–212.

[29] H. Alper, D. Bassolino, and T. Stouch, J. Chem. Phys. **98**, 9798 (1993).

[30] S. Chiu, K. Gulukota, and E. Jakobsson, in *Membrane Proteins: Structures, Interactions and Models*, edited by A. Pullman, J. Jortner, and B. Pullman (Kluwer, Dordrecht, 1992), pp. 315–338.

[31] P. Huang, J. Perez, and G. Loew, J. Biomol. Struct. Dynam. **11**, 927 (1994).

[32] R. Venable, Y. Zhang, B. Hardy, and R. Pastor, Science **262**, 223 (1993).

[33] K. Damodaran and K. Merz, Biophys. J. **66**, 1076 (1994).

[34] A. Robinson, W. Richards, P. Thomas, and M. Hann, Biophys. J. **67**, 2345 (1994).

[35] H. Berendsen, J. Postma, W. van Gunsteren, A. DiNola, and J. Haak, J. Chem. Phys. **81**, 3684 (1984).

[36] T. McIntosh, Biochemistry **25**, 4058 (1986).

[37] F. Jähnig, Biophys. J. **46**, 687 (1984).

[38] J. Nagle, Annu. Rev. Phys. Chem. **31**, 157 (1980).

[39] F. Jähnig, Biophys. J. (in press).

[40] T. L. Hill, *Introduction to Statistical Mechanics* (Dover, Mineola, NY, 1986).

[41] M. J. Ruocco and G. G. Shipley, Biochim. Biophys. Acta **691**, 309 (1982).

[42] Y. Inoko and T. Mitsui, J. Phys. Soc. Jpn. **44**, 1918 (1978).

[43] M. J. Janiak, D. M. Small, and G. G. Shipley, Biochemistry **15**, 4575 (1976).

[44] J. P. Ryckaert, G. Ciccotti, and H. J. C. Berendsen, J. Comput. Phys. **23**, 327 (1977).

[45] L. Lis, M. McAlister, N. Fuller, and R. Rand, Biophys. J. **37**, 657 (1982).

[46] B. Lewis and D. Engleman, J. Mol. Biol. **166**, 211 (1983).

[47] H. Schindler and J. Seelig, Biochemistry **14**, 2283 (1975).

[48] R. Pace and S. Chan, J. Chem. Phys. **76**, 4217 (1982).

[49] L. De Young and K. Dill, Biochemistry **27**, 5281 (1988).

[50] R. Thurmond, S. Dodd, and M. Brown, Biophys. J. **59**, 108 (1991).

[51] J. Nagle, Biophys. J. **64**, 1476 (1993).

[52] R. Rand and V. Parsegian, Biochim. Biophys. Acta **988**, 351 (1989).

[53] S. Church, D. Griffiths, R. Lewis, R. McElhaney, and H. Wickman, Biophys. J. **49**, 597 (1986).

[54] K. Gawrisch *et al.*, Biophys. J. **61**, 1213 (1992).

[55] J. Nagle and M. Wiener, Biochim. Biophys. Acta **942**, 1 (1988).

[56] M. Wiener and S. White, Biophys. J. **61**, 434 (1992).

[57] R. Flewelling and W. Hubbell, Biophys. J. **49**, 541 (1986).

[58] S. Simon and T. McIntosh, Proc. Natl. Acad. Sci. USA **86**, 9263 (1989).

[59] J. Seelig, Q. Rev. Biophys. **10**, 353 (1977).

[60] J. Seelig and A. Seelig, Q. Rev. Biophys. **13**, 19 (1980).